



Optimum design of cam-roller follower mechanism using a new evolutionary algorithm

Ferhat Hamza^{1,2} · Hammoudi Abderazek^{1,2} · Smata Lakhdar^{1,3} · Djeddou Ferhat^{1,2} · Ali Rıza Yıldız⁴

Received: 30 April 2018 / Accepted: 9 August 2018 / Published online: 20 August 2018
© Springer-Verlag London Ltd., part of Springer Nature 2018

Abstract

The optimum design of a cam mechanism is a very interesting problem in the contact mechanics today, due to the alternative industrial applications as a mechanism of precision. In this paper, a new evolutionary algorithm called modified adaptive differential evolution (MADE) is introduced for multi-objective optimization of a cam mechanism with offset translating roller follower. The optimization procedure is investigated for three objectives among them minimum congestion, maximum efficiency, and maximum strength resistance of the cam. To enhance the design quality of the mechanism in the optimization process, more geometric parameters and more design constraints are included in the problem formulation. In order to validate the developed algorithm, three engineering design problems are solved. The simulation results for the tested problems indicate the effectiveness and the robustness of the proposed algorithm compared to the various existed optimization methods. Finally, the optimal results obtained for the case study example provide very useful decisions for a cam mechanism synthesis.

Keywords Cam mechanism · Roller follower · Constrained optimization · Differential evolution algorithm

1 Introduction

Cam follower is one of the simplest and the most important mechanisms found in modern machinery today. It is widely used in mechanical devices and machines especially those of the automatic type, such as printing presses, textile machinery, gear-cutting machines, screw machines, and automobile engines. However, the main drawback of this mechanism is the direct contact between the cam and the follower. This contact induces a load torque on the cam due to friction which causes a loss of energy dissipated as heat in the two parts of contact. The roller improves the transmission efficiency of the system by reducing the friction, but increases the congestion of the

mechanism in the same time. Therefore, the cam size minimization is often the primary objective in the designing process of cam mechanism. Additionally, the requirement of high system performance implies the consideration of the cam resistance and the cam profile determination to improve the desired motion accuracy and hence, optimizing the robustness of the mechanism.

In the field of the cam-follower design, various researches have been reported [1, 2]. However, most of these works have not deal with the design of the mechanism in detail. Therefore, more research is needed in this field, especially with the great development of computing technology and optimization methodologies. During the last few decades, the optimal design of cam mechanism has been a subject of many research publications where various methods are considered. Based on iterative numerical methods, Terauchi and El-Shakery [3] used the Regula-Falsi and Newton-Raphson methods to minimize the size of cam-roller follower mechanism under contact-stress constraints. Bouzakis et al. [4] employed a non-linear programming approach to optimize the dimensions of cam by considering constructive and functional requirements of the mechanism. For constraint treatment, the exterior penalty function has been used by the authors. Carra et al. [5] investigated the synthesis of cams with negative radius roller follower by using numerical analysis to minimize the pressure

✉ Ferhat Hamza
hamzaferhat8@univ-setif.dz

¹ Institute of Optics and Precision Mechanics, University Setif 1, 19000 Setif, Algeria

² Applied Precision Mechanics Laboratory, Setif, Algeria

³ Physics and Mechanics of Metallic Materials Laboratory, Setif, Algeria

⁴ Department of Automotive Engineering, Uludağ University, Görükle, Bursa, Turkey

angle. In their work, they studied and discussed the influence of the different variables on undercutting and pressure angle problems.

Some more advanced techniques such as genetic algorithm (GA) has been applied for optimizing the cam mechanism design. The GA has been used by Lampinen [6] for preliminary cam shape design and optimization of cam-operated mechanisms. Tsiafif et al. [7] proposed a multi-objective GA to select the optimal design parameters for cam mechanism with translating roller follower. This optimization approach was applied to find the set of Pareto optimal solutions with respect to the afore-mentioned objective functions. The same authors [8] employed also the GA approach to optimize the design parameters of a disk cam mechanism with translating flat-face follower. Three objectives have been considered by the authors. Later on, Flores [9] formulated a computational approach for design optimization of disk cam mechanisms with eccentric translating roller followers. The author employed the `fmincon` function of MATLAB® to solve this problem.

Recently, Hidalgo-Martinez et al. [10] developed an optimization procedure to perform the synthesis of cam mechanism with negative radius follower using Bézier curves. In the same way, Hidalgo-Martinez and Sammiguel-Rojas [11], also based on Bézier curves, investigated the synthesis of cam mechanisms with single and double flat-faced translating followers to minimize the sliding velocities. They discussed the influence of this parameter on the friction losses and the fatigue life for this kind of cam mechanisms. More recently, Jana and Bhattacharjee [12] developed a multi-objective GA to solve the design optimization problem for cam follower mechanism with simple and double harmonic profiles. The kinematic design variables, aimed to be optimized, are the angle of rotation, maximum lift of the follower and angle for maximum follower lift.

The main purpose of the present paper is to synthesize a cam mechanism with eccentric translating roller follower based on optimization approach by using a new evolutionary algorithm called MADE. Unlike previous studies, in this work, the design quality of the cam mechanism is improved by considering more geometric parameters and design constraints during the optimization procedure. The optimization problem is simultaneously formulated for three objectives: minimizing the cam size, maximizing the efficiency of the mechanism, and maximizing the cam mechanical resistance. The effectiveness of the proposed algorithm is verified by optimizing three constrained engineering design problems including three bar truss design, spring design, and welded beam design.

Thus, the organization of the remaining paper is as follows: the formulation of optimization problem, objective function, constraints, and design variables is described in Section 2. In Section 3, the different steps of classical DE algorithm are

briefly exposed. The developed MADE algorithm is presented in Section 4 and validated in Section 5. In Section 6, an application example is presented and used to discuss the main assumptions and procedures adopted throughout this work. Finally, the conclusion is given in Section 7.

2 Problem formulation of the cam mechanism

A schematic view of a cam mechanism with offset translating roller follower is shown in Fig. 1. According to previous studies [7, 9, 13], the optimum design of this mechanism can be achieved by considering three major parameters that influence the cam design process, namely the base circle radius of the cam R_b , the roller radius R_g , and the offset of the follower e . However, it is of great importance to consider other parameters that may improve the system performance. Particularly, those associated with the geometric elements of the mechanism such as the cam thickness, distance between the cam center, and the follower bearing, and the length of follower bearing.

Consequently, the main contribution of this study is to propose a global optimization procedure by considering additional geometric parameters that influence the design quality of cam mechanism with eccentric translating roller follower. The optimization problem is formulated as a multi-objective while observing several constraints on performance and resistance

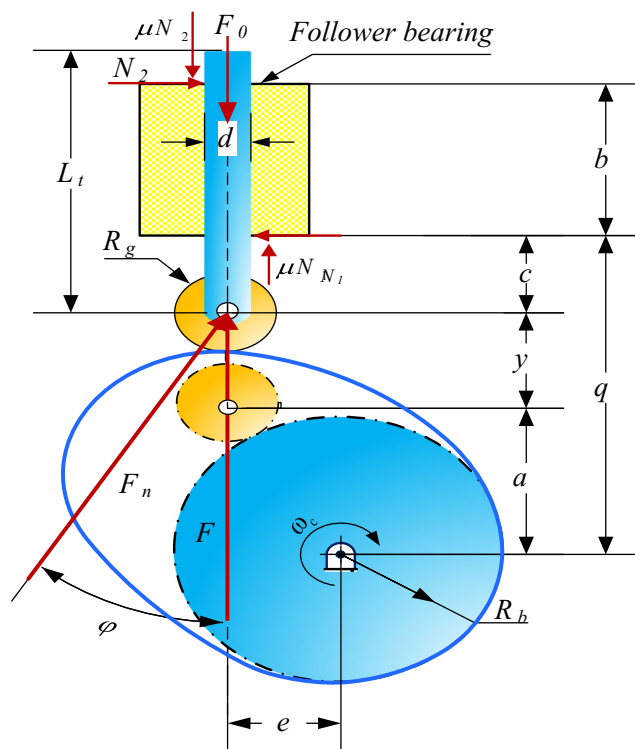


Fig. 1 Cam mechanism with offset translating roller follower

indicators, as well as geometric conditions. In the following, the objective functions, constraints, and design variables will be detailed.

2.1 Objective functions

The cam mechanism with eccentric translating roller follower must be designed for minimum congestion, maximum efficiency, and maximum strength resistance of the cam. Mathematically, the objective function can be expressed as

$$Min : f(x) = \beta_1(R_b + t) + \beta_2 \times T_{max} + \beta_3 \times \sigma_{Hmax} \quad (1)$$

where $\beta_i (i = 1, 2, 3)$ are the weighting factors of the objective function that depend on the specific problem to be solved, and x is the vector of the design variables.

From Eq. 1, the first goal is the cam size minimization. This latter is defined according to the base circle radius R_b and thickness of the cam t . The second objective is to reduce the maximum input torque required to drive the cam T_{max} which is directly increasing the mechanical efficiency. The last objective is the maximum contact stress σ_{Hmax} between the cam and the follower which should be minimized. The instantaneous input torque is given by [14] as follows:

$$T = F \times y' \quad (2)$$

where F is the force of the cam on the roller follower, and y' is the first derivative of the follower displacement with respect to the cam angle.

2.2 Constraints

The above objective functions are subjected to ten design constraints. In this section, each constraint is given in detail.

- The first two constraints are imposed to simplify the mechanism assembly (Fig. 1):

$$g_1(x) = e - R_g \geq 0 \quad (3)$$

$$g_2(x) = R_b - e \geq 0 \quad (4)$$

- In order to ensure the correct operation of the mechanism during the high dwell of the follower, the roller should not touch the follower bearing. So, the following constraint should be added to avoid the contact (Fig. 1).

$$g_3(x) = q - \alpha - h - R_g \geq 0 \quad (5)$$

where h is the lift of the follower, and q is the distance between the cam center and the follower bearing. The α parameter is calculated as

$$\alpha = \sqrt{(R_g + R_b)^2 - e^2} \quad (6)$$

- On the other hand, during the low dwell, the follower level should not be lower than the level of bearing to avoid any contact between the external mass and this latter. Mathematically, the constraint can be formulated as

$$g_4(x) = L - (q - \alpha) - b \geq 0 \quad (7)$$

where L is the length of the follower and b is the length of the follower bearing, as shown in Fig. 1.

- In order to guarantee the proper operation of the mechanism, two constraints are imposed on the pressure angle. These are the maximum allowed values for the rise and the return periods, which stated as [9]

$$g_5(x) = -\max|\varphi_{Rise}| + 30^\circ \geq 0 \quad (8)$$

$$g_6(x) = -\max|\varphi_{Return}| + 45^\circ \geq 0 \quad (9)$$

The pressure angle is given as follows [14]:

$$\varphi = \tan^{-1} \left(\frac{y' - e}{y + a} \right) \quad (10)$$

- To avoid undercutting as well as to ensure the desired movement of the mechanism, two other constraints are imposed on the curvature radius of the pitch curve ρ . When the cam is on the convex part, the minimum positive radius of curvature ρ_{min} should be greater or equal to the roller radius R_g [15]. When the cam is on the concave part, the absolute value of the minimum curvature radius $|\rho_{min}|$ should be too greater than R_g [16]. Thus, the two constraints are written as the following:

For $\rho > 0$,

$$g_7(x) = \rho_{min} - R_g \geq 0 \quad (11)$$

For $\rho < 0$,

$$g_8(x) = |\rho_{min}| - R_g - r \geq 0 \quad (12)$$

where r is a positive constant to control the variation of the curvature radius for the concave part of the cam. The curvature radius of the pitch curve ρ can be calculated as [17]

$$\rho = \frac{\sqrt{((R_b + R_g + y)^2 + y')^3}}{(R_b + R_g + y)^2 + 2y' - (R_b + R_g + y)y''} \quad (13)$$

where y'' is the second derivative of the follower displacement with respect to the cam angle.

- To ensure the mechanical resistance of the cam, the maximum contact stress σ_{Hmax} should be less or equal to the permissible contact stress σ_{HP} . Mathematically, the constraint is expressed as

$$g_9(x) = \sigma_{HP} - \sigma_{Hmax} \geq 0 \quad (14)$$

The maximum contact stress applied on the cam is calculated as follows [15]:

$$\sigma_{Hmax} = 0.564 \sqrt{\frac{F_n \times (R_b + R_g)}{t \times (R_b \times R_g) \times [(1-\nu_1^2)/E_1 + (1-\nu_2^2)/E_2]}} \quad (15)$$

where F_n is the normal force between the cam surface and the roller follower [18]:

$$F_n = \frac{P}{\left[1 - \mu \left(\frac{2C + b}{b}\right) \tan(\varphi)\right] \cos(\varphi)} \quad (16)$$

where P is the total force acting on the follower. This force is the algebraic sum of the external applied force F_0 , the inertial force F_i and the spring force F_s . μ is the coefficient of friction between the follower and its bearing, $C = q - (a + y)$ (Fig. 1). ν_1, ν_2 are Poisson coefficients and E_1, E_2 are the elasticity modulus of the material of cam and roller follower respectively.

- The last constraint is the mechanical efficiency of the system. The power transmission of the mechanism should be done with a minimum loss of energy which due mainly to friction and pressure angle. Thereby, the constraint on the minimal limit of energy loss is established as follows:

$$g_{10}(x) = \eta_{min} - 0.90 \geq 0 \quad (17)$$

The instantaneous efficiency is given by the report of the total force P on the required force to lift the follower F . Its expression may be written as

$$\eta = 1 - \mu \left(\frac{2C + b}{b}\right) \tan(\varphi) \quad (18)$$

2.3 Design variables

From the problem formulation, it is clear that the design optimization of a cam mechanism is affected by the geometric parameters proposed previously, which are conflicting with each other. When the cam thickness t is increased, the resistance of the cam is improved (third objective) due to the direct reducing in the contact stress. But at the same time, the cam size becomes greater, which does not serve the first objective. It is then necessary to select an optimum

value of this parameter. Also, the reduction of the distance q allows the decrease of the input torque T by increasing the mechanical efficiency η . It means that we play on the second term of the objective function, but at the same time the constraint g_3 should be respected. On the other hand, the length of the follower bearing b has a certain influence on the input torque and on the constraint g_4 . In addition, the two latter parameters have a direct influence on the normal force F_n and thus affecting the contact stress (third term of the objective function).

Based on the above analysis, the final optimization model of the cam mechanism design is developed for six design variables. They are the cam base circle radius R_b , roller radius R_g , follower offset e , cam thickness t , distance between the cam center and the follower bearing q , and follower bearing length b . All the design variables are continuous.

3 Basic steps of differential evolution algorithm

DE algorithm is one of the most efficient evolutionary algorithms (EAs) which was firstly proposed by Storn and Price [19] for real parameter optimization. Like other EAs, DE is a population-based optimization algorithm. The classical DE algorithm can be divided into four steps, which are the initialization, mutation, crossover, and selection. During the initialization phase, the population NP is randomly created within the feasible boundary constraints of each decision variable $x_{i,j}^{G=0} = (x_{1,j}^{G=0}, \dots, x_{D,j}^{G=0})$, $i = 1, \dots, D$ and $j = 1, \dots, NP$. D denotes the number of design variables.

After the initialization step, DE uses the mutation operation to create a mutant vector for each target vector. The DE/rand/2/bin strategy is the most used one, where bin denotes the binomial crossover operator. The mutation vector can be calculated as follows:

$$v_{i,j}^{G+1} = x_{i,r_1}^G + F_1 \times (x_{i,r_2}^G - x_{i,r_3}^G) + F_2 \times (x_{i,r_4}^G - x_{i,r_5}^G) \quad (19)$$

where r_1, r_2, r_3, r_4 , and r_5 are integer indices randomly chosen within the range $[1, \dots, NP]$, different from each other and also different from the index j . F_1 and F_2 are the scaling factors and G denotes the generation number.

In the binomial crossover, the trial vector $u_{i,j}^{G+1}$ is generated using the target and mutated vectors as

$$u_{i,j}^{G+1} = \begin{cases} v_{i,j}^{G+1}, & \text{if } (\text{rand}_{i,j}[0, 1] \leq Cr) \vee (i == i_{rand}) \\ x_{i,j}^G, & \text{otherwise} \end{cases} \quad (20)$$

where i_{rand} is a randomly integer chosen in $[1, \dots, D]$. $\text{rand}_{i,j}$ is a uniformly distributed random number between 0 and 1.

Table 1 Design variables, objective function, and constraint values for engineering design problems

| | Three bar truss | Tension spring | Welded beam |
|-----------|-------------------|------------------|----------------|
| x_1 | 0.788675136255355 | 0.05168906073973 | 0.205729639786 |
| x_2 | 0.408248285767141 | 0.35671773154718 | 3.470488665628 |
| x_3 | – | 11.2889662354172 | 9.036623910357 |
| x_4 | – | – | 0.205729639786 |
| $g_1(x)$ | 0 | 0 | –1.8189894E–12 |
| $g_2(x)$ | –1.46410162047705 | 0 | 0 |
| $g_3(x)$ | –0.53589837952295 | –4.0537856140377 | 0 |
| $g_4(x)$ | – | –0.7277288051420 | –3.43298420860 |
| $g_5(x)$ | – | – | –0.08072963978 |
| $g_6(x)$ | – | – | –0.23554032258 |
| $g_7(x)$ | – | – | –2.7284841E–12 |
| f_{min} | 263.895843376468 | 0.01266523278831 | 1.724852308597 |

During the selection step, the target vector $x_{i,j}^G$ is compared with the trial vector $u_{i,j}^{G+1}$ and the better one will be selected to enter the next generation according to their fitness value:

$$x_{i,j}^{G+1} = \begin{cases} u_{i,j}^{G+1} & \text{if } f(u_{i,j}^{G+1}) \leq f(x_{i,j}^G) \\ x_{i,j}^G & \text{otherwise} \end{cases} \quad (21)$$

If the stopping criterion is satisfied, the computation is terminated. Otherwise, the step mutation, crossover, and selection are repeated.

4 Modified adaptive differential evolution

The proposed method can be considered as an improved version of the adaptive mixed differential evolution (AMDE) [20]. Specifically, the AMDE algorithm has been developed to select the optimal geometry parameters of a cylindrical spur gear. In addition, to avoid the manual tuning of the mutation and crossover values, the method is based on self-adaptive mechanism jDE [21]. For further details about the AMDE method, the interesting reader may refer to [20].

In the present paper, the MADE algorithm is reinforced by using the superiority of feasible points mechanism,

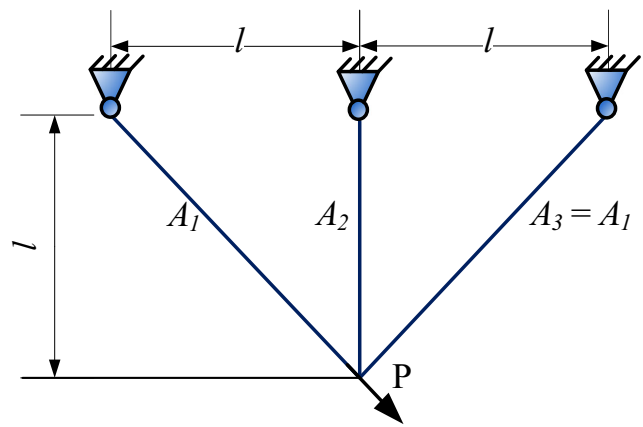


Fig. 2 Three bar truss design

proposed by Deb [22], in the selection phase instead the conventional one to improve the search capability of the variant, where the Deb’s approach is based on three selection scenarios when comparing between the target vector $x_{i,j}^G$ and the trial vector $u_{i,j}^{G+1}$. The sequence of each criterion is given as follows: when two solutions are in the feasible region, the one with the better fitness value is selected; secondly, if one solution is feasible and the other is infeasible, the feasible one is preferred; the last scenario is among two infeasible solutions; the one with the small constraint violation value is chosen. It may be noted that in this work, we will deal only with problems of continuous type.

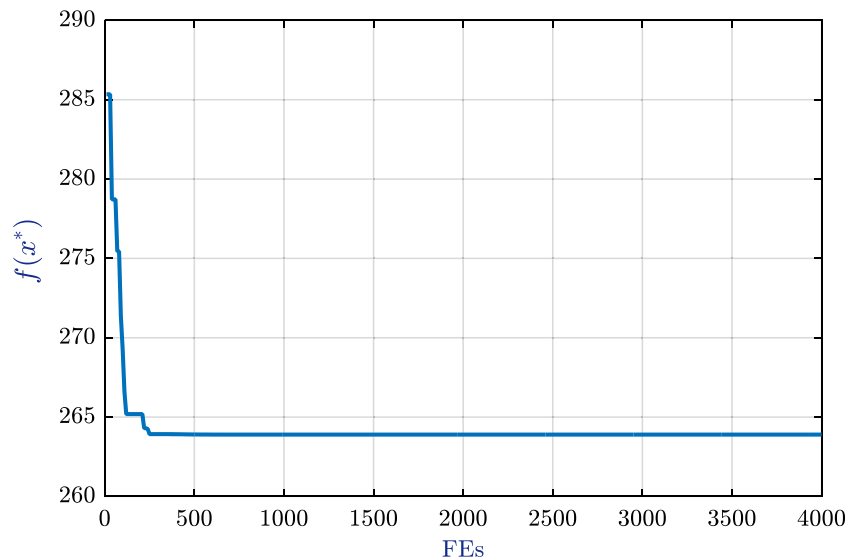
5 Evaluation of MADE approach

In order to evaluate the performance of the proposed approach, three real-world engineering optimization problems are selected which are three bar truss design, tension spring design, and welded beam design problem. The mathematical formulation of the benchmark engineering design problems are presented in Appendix. The parameters of the jDE for the problems are as follows: initialization process sets $F_1= 0.8$, $F_2= 0.5$, $Cr= 0.5$, $\tau_1= 0.5$, $\tau_2= 0.2$, and $\tau_3= 0.1$. NP is chosen in range [4D 10D] and the number of function evaluations (FEs) is given in Table 2. Moreover, for each problem, 50 independent runs are performed and statistical results are provided including

Table 2 Statistical results obtained by MADE for the three engineering design problems

| Problem | Best | Mean | Worst | SD | FEs |
|-----------------|-------------------|-------------------|-------------------|------------|--------|
| Three bar truss | 263.8958433764684 | 263.8958433764685 | 263.8958433764686 | 2.7005E–13 | 4000 |
| Tension spring | 0.012665232788319 | 0.012665232788320 | 0.012665232788323 | 5.8876E–16 | 20,000 |
| Welded beam | 1.724852308597364 | 1.724852308597365 | 1.724852308597366 | 9.6318E–16 | 18,000 |

Fig. 3 Objective function value respect to number FEs for three bar truss design



best, mean, worst, and standard deviation. The MADE algorithm is implemented in MATLAB® and the optimization runs are executed on a PC i5 with a 2.2 GHz and 4 GB of RAM memory.

The mentioned problems are recently solved by using several approaches. MADE algorithm is compared with following metaheuristics: AMDE [20], rank-iMDDE [23], constrained optimization based on a modified DE (COMDE) [24], multiple trial vector-based DE (MDDE) [25], water cycle algorithm (WCA) [26], differential evolution with level comparison (DELIC) [27], ϵ -constrained differential evolution algorithm with a novel local search operator (ϵ DE-LS) [28], and social-spider algorithm (SSO-C) [29].

The optimal results obtained by MADE algorithm for the three engineering problems are presented in Table 1. In addition, the statistical results are summarized in Table 2. According to the two tables, it is clearly observed that the developed algorithm can obtain the feasible global optimal solution for all engineering problems with small function evaluations number, no more than 20,000 in case of the welded beam design problem. This indicates that the proposed

MADE is very effective in solving the engineering problems in terms of solution quality, convergence speed, and robustness.

5.1 Three bar truss design

The first problem deals with the design of a three-bar truss structure [30] in which the volume is to be minimized and subjected to stress constraints. The design variables are the cross-sectional areas A_1 (x_1) and A_2 (x_2) as shown in Fig. 2. Figure 3 shows the convergence of MADE to the best solution for the three-bar truss problem.

This problem has been solved by AMDE, rank-iMDDE, COMDE, DSS-MDE, WCA, DELIC, and ϵ DE-LS. The results of these algorithms are shown in Table 3; a result in italic means a better solution obtained. In terms of the standard deviation, rank-iMDDE is the best one, followed by ϵ DE-LS, DELIC, MADE, AMDE, and COMDE. However, MADE and AMDE show superiority in terms of FEs among the compared algorithms.

Table 3 Comparison with other state-of-the-art algorithms on three bar truss problem

| Method | Best | Mean | Worst | SD | FEs |
|------------------|-------------------|-------------------|-------------------|------------|--------|
| MADE | 263.8958433764684 | 263.8958433764685 | 263.8958433764686 | 2.7005E-13 | 4000 |
| AMDE | 263.8958433764684 | 263.8958433764685 | 263.8958433764686 | 2.7441E-13 | 4000 |
| rank-iMDDE | 263.8958434 0 | 263.8958434 | 263.8958434 | 0.00E+00 | 4920 |
| COMDE | 263.8958434 | 263.8958434 | 263.8958434 | 5.34E-13 | 7000 |
| DSS-MDE | 263.8958433 | 263.8958436 | 263.8958498 | 9.70E-07 | 15,000 |
| WCA | 263.895843 | 263.895843 | 263.895843 | 8.71E-05 | 5250 |
| DELIC | 263.8958434 | 263.8958434 | 263.8958434 | 4.34E-14 | 10,000 |
| ϵ DE-LS | 263.895843376468 | 263.895843376468 | 263.895843376468 | 2.3206E-14 | 15,000 |

Fig. 4 Tension spring design

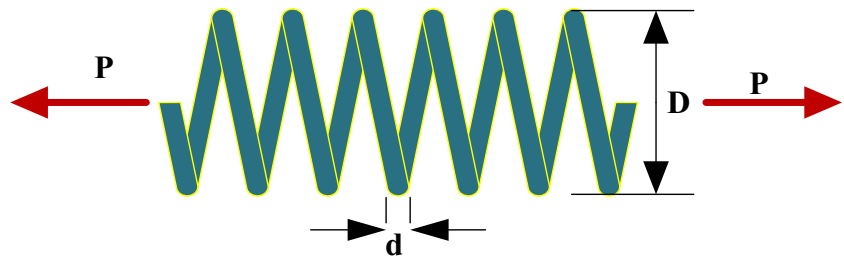
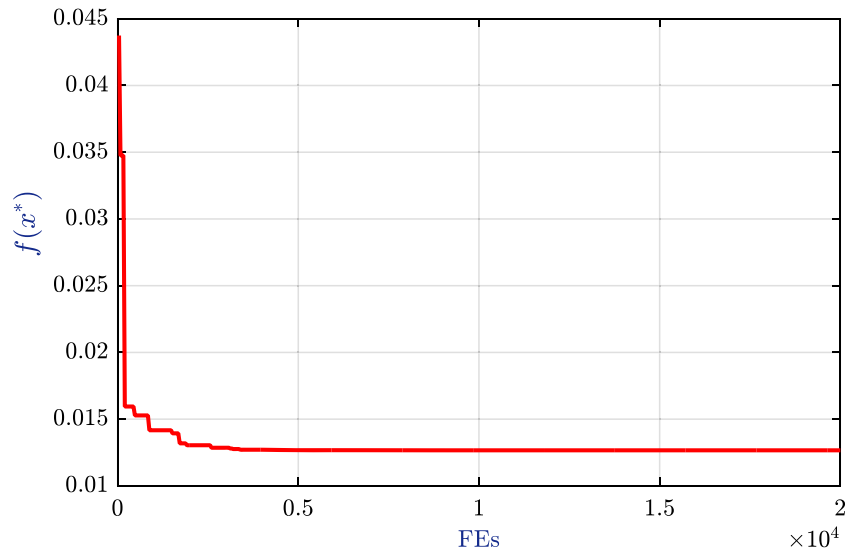


Fig. 5 Objective function value respect to number FEs for tension spring design



5.2 Tension spring design problem

The purpose is to minimize the volume of the tension spring [31], as shown in Fig. 4, subjected to four constraints on shear stress, surge frequency, minimum deflection, and limits on outside diameter and on design variables. There are three continuous design variables including the wire diameter d (x_1), the mean coil diameter D (x_2), and the number of active coils N (x_3). The convergence of MADE to the best solution for the tension spring design problem is shown in Fig. 5.

The problem has been recently solved by using several algorithms, including rank-iMDDE, COMDE, DSS-MDE, WCA, DELC, and ϵ DE-LS. The results of these algorithms are shown in Table 4. As it can be seen from the table, the best solution obtained is 0.01266523. Further, among the compared algorithms, it is observed that MADE is more robust in solving this problem with a standard deviation value of $5.8876E-16$. In addition, the proposed variant obtains the best results compared with the seven algorithms in terms of best, mean, and worst solutions.

Table 4 Comparison with other state-of-the-art algorithms on tension spring design problem

| Problem | Best | Mean | Worst | SD | FEs |
|------------------|-------------------|-------------------|-------------------|------------|--------|
| MADE | 0.012665232788319 | 0.012665232788320 | 0.012665232788323 | 5.8876E-16 | 20,000 |
| AMDE | 0.012665232788319 | 0.012665232788326 | 0.012665232788574 | 3.6617E-14 | 20,000 |
| rank-iMDDE | 0.012665233 | 0.012665264 | 0.01266765 | 2.45E-07 | 19,565 |
| COMDE | 0.012665233 | 0.012665233 | 0.012665233 | 3.09E-06 | 24,000 |
| DSS-MDE | 0.012665233 | 0.012669366 | 0.012738262 | 1.25E-05 | 24,000 |
| WCA | 0.012665 | 0.012746 | 0.012952 | 8.06E-05 | 11,750 |
| DELC | 0.012665233 | 0.012665267 | 0.012665575 | 1.30E-07 | 20,000 |
| ϵ DE-LS | 0.012665233 | 0.012665233 | 0.012665233 | 5.0075E-14 | 20,000 |

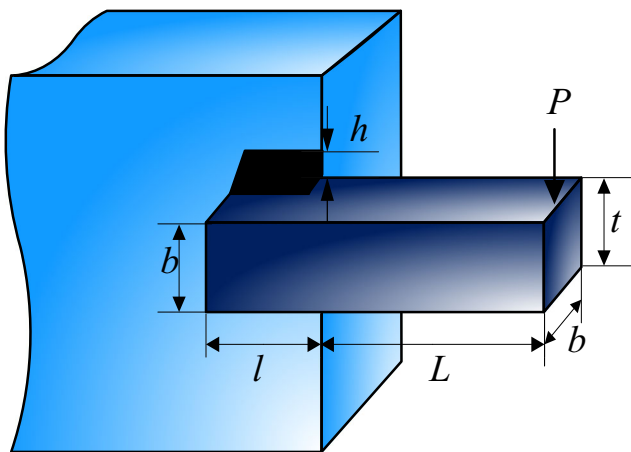


Fig. 6 Welded beam design problem

5.3 Welded beam design problem

The objective is to minimize the manufacturing cost of the welded beam [32] subjected to constraints on shear stress (τ), bending stress in the beam (σ), buckling load on the bar (Pc), end deflection of the beam (δ), and side constraints. There are four design variables as shown in Fig. 6: h (x_1), l (x_2), t (x_3), and b (x_4). The convergence graph of MADE for the welded beam design problem is plotted in Fig. 7.

MADE is compared with seven EAs in this problem. They are AMDE, rank-iMDDE, COMDE, DELC, WCA, MDDE, and SSO-C. The results of these algorithms are shown in Table 5. It can be observed from the statistical results that all the mentioned algorithms are able to find the global optimal solution. Further, MADE and rank-iMDDE provided the small standard deviation. Moreover, with the

smallest FEs, MADE is considered the most efficient among all compared methods.

6 Case study of the cam mechanism

The proposed approach is applied and evaluated for solving the cam design optimization problem with the following data. Firstly, the length of the follower L , its diameter d , and its mass M are defined under the resistance conditions which must be verified to the following compressive and buckling solicitations:

$$\begin{cases} \sigma_{c \max} \leq R_e \\ R_e \leq \sigma_b \end{cases} \quad (22)$$

where $\sigma_{c \max}$ is the maximum compressive stress, σ_b is the buckling critical limit, and R_e is the elastic limit of the follower material.

The input data for the follower and the parameters of case study example are presented in Tables 6 and 7, respectively. In addition, by following the same methodology as in [33–35], the kinematic analysis of the follower motion such as displacement, velocity, and acceleration is presented in Figs. 8, 9, and 10 respectively. Moreover, the dynamic analysis including the external force, spring force, inertial force and total force acting on the follower is given in Fig. 11. Assuming the simple harmonic motion (SHM) of the type rise-dwell-return-dwell (RDRD), the motion kinematics are given by Eqs. 23, 24, and 25 [14]:

Fig. 7 Convergence graph of MADE for welded beam design

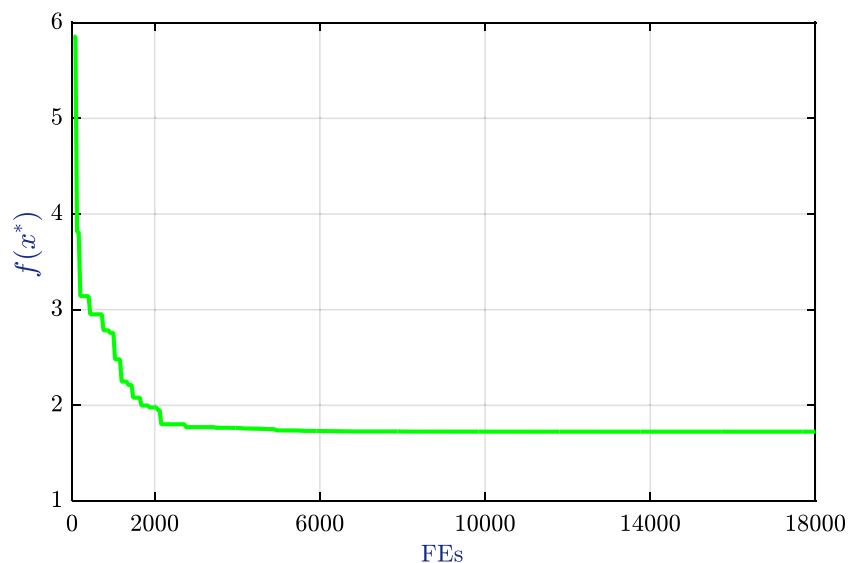


Table 5 Comparison with other state-of-the-art algorithms on welded beam design problem

| Problem | Best | Mean | Worst | SD | FES |
|------------|-------------------|-------------------|-------------------|------------|--------|
| MADE | 1.724852308597364 | 1.724852308597365 | 1.724852308597366 | 9.6318E-16 | 18,000 |
| AMDE | 1.724852308597364 | 1.724852308597365 | 1.724852308597366 | 1.1533E-15 | 18,000 |
| rank-iMDDE | 1.724852309 | 1.724852309 | 1.724852309 | 9.06E-16 | 19,830 |
| COMDE | 1.724852 | 1.724852 | 1.724852 | 1.60E-12 | 20,000 |
| DELC | 1.724852 | 1.724852 | 1.724852 | 4.10E-13 | 20,000 |
| WCA | 1.724856 | 1.726427 | 1.744697 | 4.29E-03 | 46,450 |
| MDDE | 1.725 | 1.725 | 1.725 | 1.00E-15 | 24,000 |
| SSO-C | 1.7248523085 | 1.746461619 | 1.799331766 | 2.57E-02 | 25,000 |

$$y = \frac{h}{2} \left(1 - \cos \left(\pi \frac{\theta}{\theta_{\text{Rise}}} \right) \right) \tag{23}$$

$$y' = \left(\frac{h}{2} \times \frac{\pi}{\theta_{\text{Rise}}} \right) \times \left(\sin \left(\pi \frac{\theta}{\theta_{\text{Rise}}} \right) \right) \tag{24}$$

$$y'' = \left(\frac{h}{2} \times \frac{\pi^2}{\theta_{\text{Rise}}^2} \right) \times \left(\cos \left(\pi \frac{\theta}{\theta_{\text{Rise}}} \right) \right) \tag{25}$$

where θ is the cam rotation angle and θ_{Rise} is the rise period angle. The follower characteristics are calculated for 60° rise, 130° high dwell, 140° returns, 30° low dwell, follower lift $h = 20$ mm, and cam speed $\omega_c = 2$ rad/s.

From Figs. 9 and 10, it is observed that the dwell periods have always zero velocity and zero acceleration. During the rise and the return periods, the follower velocity follows a sine function and its peak values are respectively 60 mm/s and 25.72 mm/s. The follower acceleration follows a cosine function and its peak values are, respectively 360 mm/s² and 66.12 mm/s². It can then be deduced that the motion law considered in this study provides an acceleration curve with finite values at the rise and the return periods, which leads to reduce the amplitude of the inertia force applied on the follower, as can be seen in Fig. 11. On the other hand, the spring force, which is directly related to the follower displacement, has the major contribution on the total force.

Table 6 Input data of the follower

| Input data | Values |
|---|----------------------------|
| Material density (kg/m ³) | 8027 |
| Material elastic limit R_e (MPa) | 170 |
| Follower inertial moment (mm ⁴) | $\pi \cdot \frac{d^4}{64}$ |
| d (mm) | 10 |
| L (mm) | 80 |
| M (kg) | 50.183×10^{-3} |

6.1 Results and discussions

The cam mechanism with offset roller follower translation must be designed for minimum congestion, maximum efficiency, and maximum strength resistance of the cam. There are six continuous design variables. In addition, the objectives are subjected to ten inequalities constraints, two linear and eight nonlinear. The MADE algorithm adapts a self approach to solve this problem while the used parameters are as follows: NP = 30, FES = 25,000, we conserve the same values as in Section 5 for the scaling factors and crossover factor.

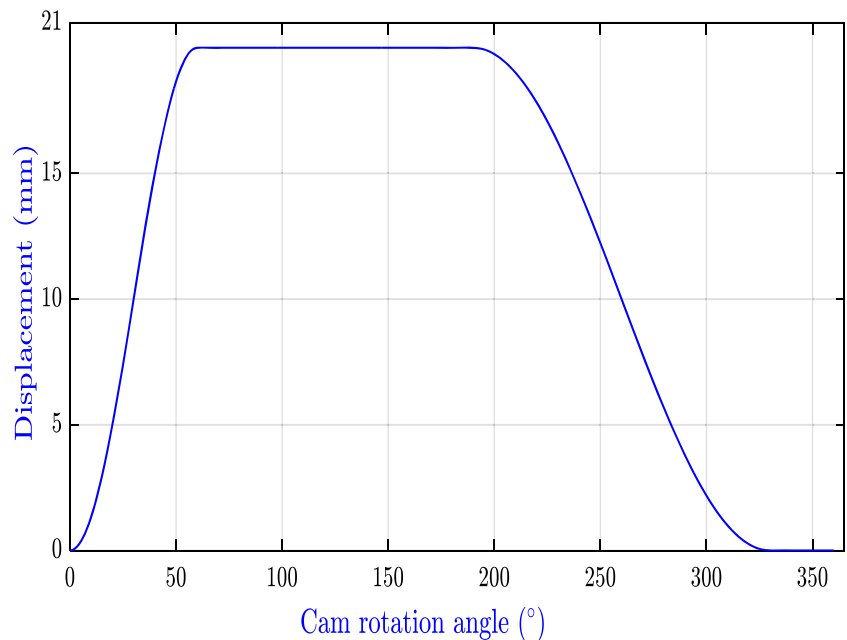
In order to solve this problem, the weighted sum method is used [36]. The basic idea of this method is to convert the multi-objective problem to the single one by using the weighting factors. In the present case, they are taken as, $\beta_1 = 0.8$, $\beta_2 = 0.1$, and $\beta_3 = 0.1$. The upper and the lower variable limits are as follows: $20 \leq R_b \leq 60$, $0 \leq R_g \leq 20$, $0 \leq e \leq 20$, $0 \leq t \leq 20$, $50 \leq q \leq 130$, $25 \leq b \leq 55$.

The statistical results obtained by the developed version are summarized in Table 8 (50 runs). The graphical convergence speed of MADE to the best solution for the cam mechanism

Table 7 Input parameters of the case study

| Input data | Values |
|--|-------------------|
| E_1 (MPa) | 2.1×10^5 |
| E_2 (MPa) | 2×10^5 |
| ν_1 | 0.28 |
| ν_2 | 0.265 |
| σ_{adm} (MPa) | 235 |
| μ | 0.1 |
| Spring rate k ($\frac{N}{mm}$) | 1.2 |
| Initial deflection of the spring δ (mm) | 8 |
| r (mm) | 10 |
| F_0 (N) | 30 |

Fig. 8 Displacement diagram of the follower motion



problem is given in Fig. 12. From Table 8, the best solution given by the MADE is $x^*=[28.633568856151, 9.3006758804433, 9.3006758804458, 9.8395981706191, 67.0770861444, 48.6993241195]$, corresponding to the objective function value $f = 217.70907431$. In addition, the developed algorithm offered a small standard deviation value ($1.0809E-08$) which confirms the robustness of the MADE in solving this problem. Moreover, from Fig. 12, it is clear that MADE version converged rapidly

and can achieve the near-optimum within only in 250 iterations.

The optimum design variables obtained through the optimization procedure are used to plot the evolution of pressure angle, radius of curvature, and contact stress in function of the cam rotational angle, as shown in Figs. 13, 14, and 15 respectively. According to Fig. 13, it is clear that both values of φ_{Rise} and φ_{Return} are well below the allowable limits 30° and 45° respectively. This is due to the fact

Fig. 9 Velocity diagram of the follower motion

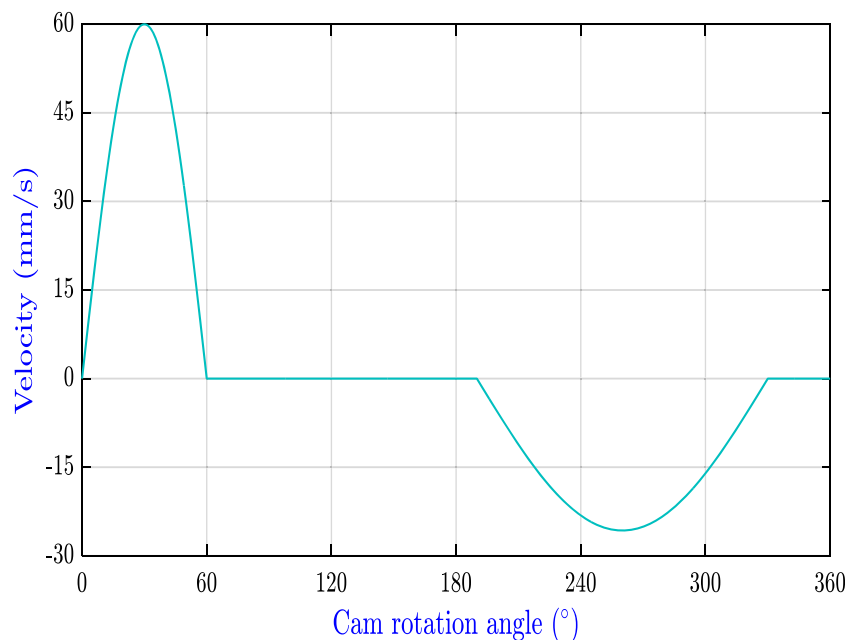
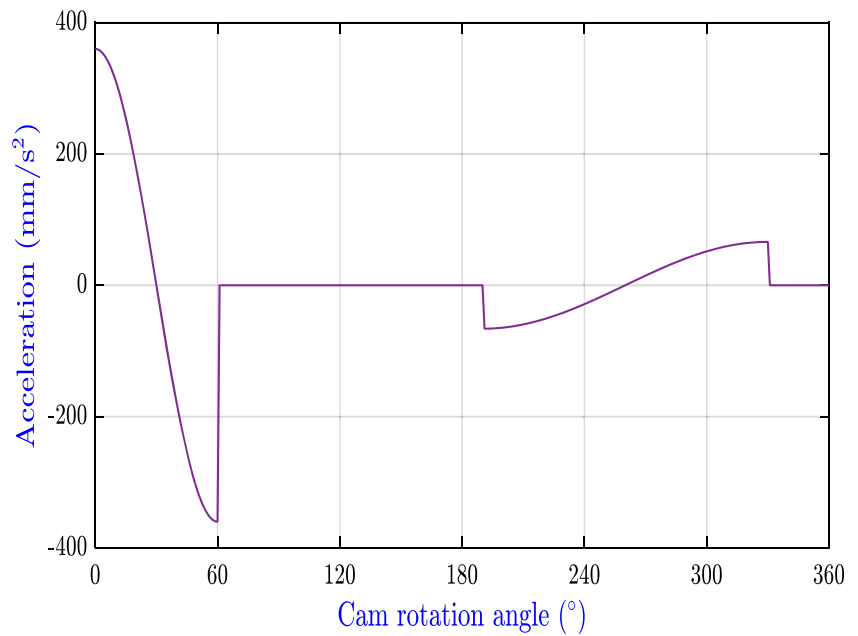


Fig. 10 Acceleration diagram of the follower motion



of second term of the objective function which indicates that reducing the input torque leads to an increase in the efficiency and a reduction of pressure angles, thereby confirming the desired performance of the mechanism. Figure 14 shows that the minimum values of the curvature radius for convex and concave parts of the optimized cam are satisfied (constraints g_7 and g_8 respectively in Table 8). Following the same logic, we can deduce from Fig. 15 that the large gap between the maximum contact stress applied on the cam and its allowable limit is due to the influence of

third term of the objective function, which indicates a good strength of the cam (g_9).

In addition, the risk of the contact between the roller and the follower bearing during the high dwell of the follower is avoided with a safety distance equal to 1.00 mm, (constraint g_3 of Table 8). For cons, the value found for the constraint g_4 presents the safety height between the follower and its bearing during the low dwell. Finally, the obtained optimal cam profile is given in Fig. 16.

Fig. 11 Evolution of external, inertial, spring, and total forces respect to cam rotation angle

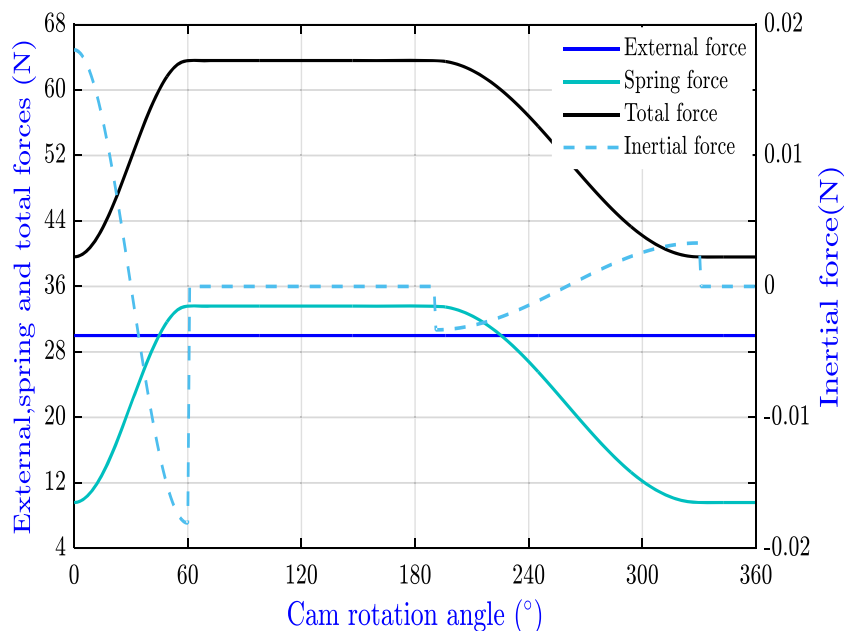


Table 8 Global optimal results of the cam-roller follower mechanism

| Optimization method | MADE |
|---------------------|------------------|
| Best | 217.70907431416 |
| $R_b(\text{mm})$ | 28.633568856151 |
| $R_g(\text{mm})$ | 9.3006758804433 |
| $e(\text{mm})$ | 9.3006758804458 |
| $t(\text{mm})$ | 9.8395981706191 |
| $q(\text{mm})$ | 67.077086144401 |
| $b(\text{mm})$ | 48.699324119543 |
| $g_1(x)$ | 2.479794147E-12 |
| $g_2(x)$ | 19.332892975705 |
| $g_3(x)$ | 1.0000028484105 |
| $g_4(x)$ | 1.0000033129137 |
| $g_5(x)$ | 5.7885443809810 |
| $g_6(x)$ | 18.746593846853 |
| $g_7(x)$ | 13.387625392705 |
| $g_8(x)$ | 8.3376253927057 |
| $g_9(x)$ | 77.566177908637 |
| $g_{10}(x)$ | 2.076117056E-14 |
| Mean | 217.709074327487 |
| Worst | 217.709074371881 |
| SD | 1.0809E-08 |

mechanism was optimized regarding the minimum cam size, maximum efficiency, and maximum cam strength resistance. The optimization problem was subjected to constraints on performance indicators such as pressure angle, efficiency, and resistance indicators (radius of curvature and contact stress), as well as geometric conditions. The design variables considered in the optimization process were of a continuous nature in a total of six, which select numerous geometric parameters of the mechanism elements. In order to solve this multi-objective problem, the weighted sum method was used, where the weighting factors were chosen in accordance with the importance of each objective. The results found through the design example showed that the optimum synthesis has been performed by an excellent efficiency and a sufficient durability.

Furthermore, the effectiveness of the proposed algorithm has been verified by solving three well-known problems which are the three bar truss, tension spring, and welded beam design. The obtained results for the engineering problems demonstrated the effectiveness and the robustness of the proposed approach compared to the existing optimization methods. The obtained results for the case study of the cam mechanism confirmed the efficiency of MADE in solving the real engineering complex problems. For future research directions, the MADE algorithm will be used for further applications as well as other types of cam mechanism synthesis. In addition, an experimental study to test and to validate the performance of the algorithm is recommended.

7 Conclusion

In this work, a new efficient algorithm called MADE was presented for a global optimum design of a cam mechanism with offset roller follower translation. The

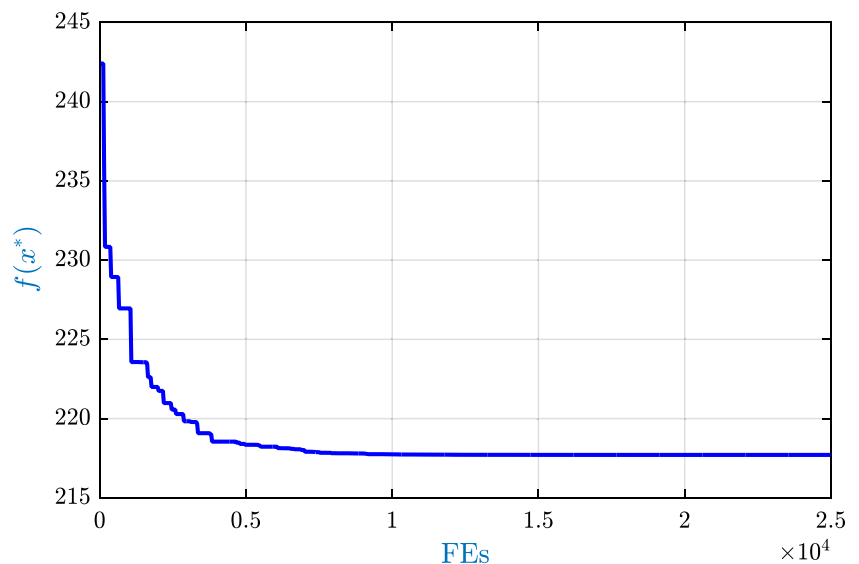
Fig. 12 Convergence graph of MADE for the case study

Fig. 13 Evolution of the pressure angle

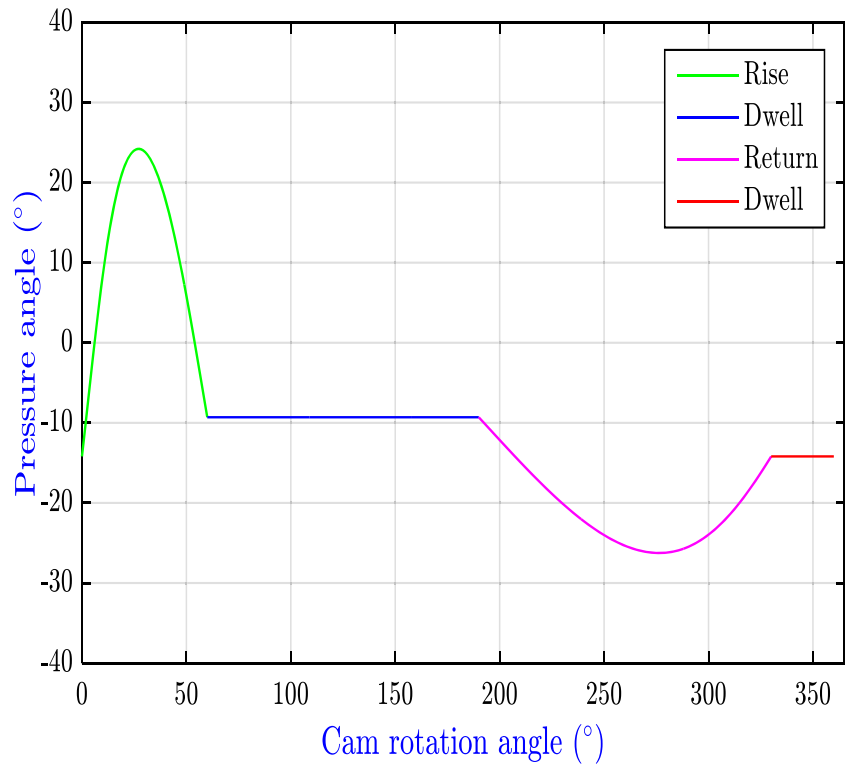


Fig. 14 Evolution of the curvature radius

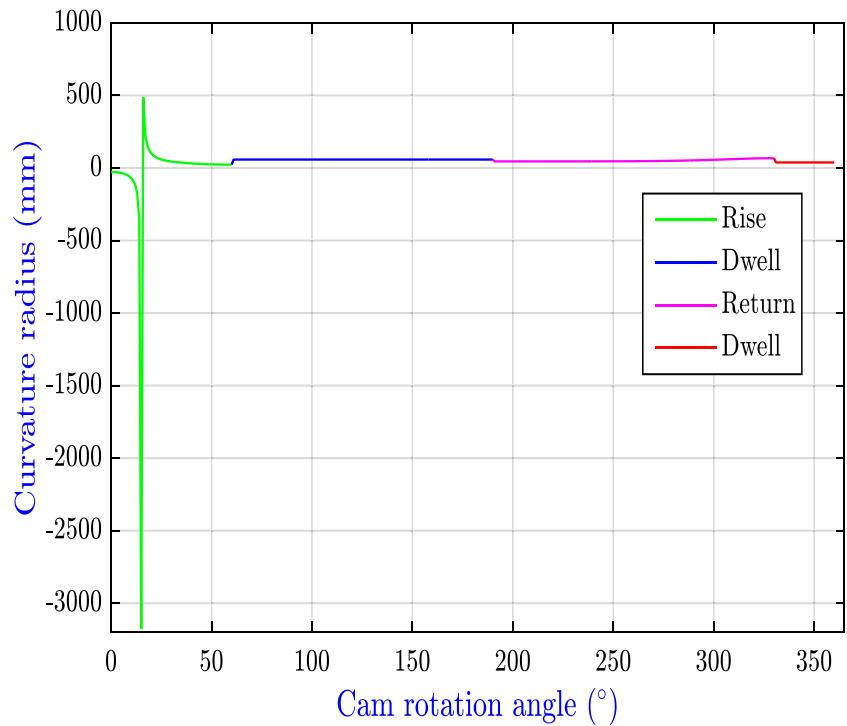


Fig. 15 Evolution of the Hertzian contact stress

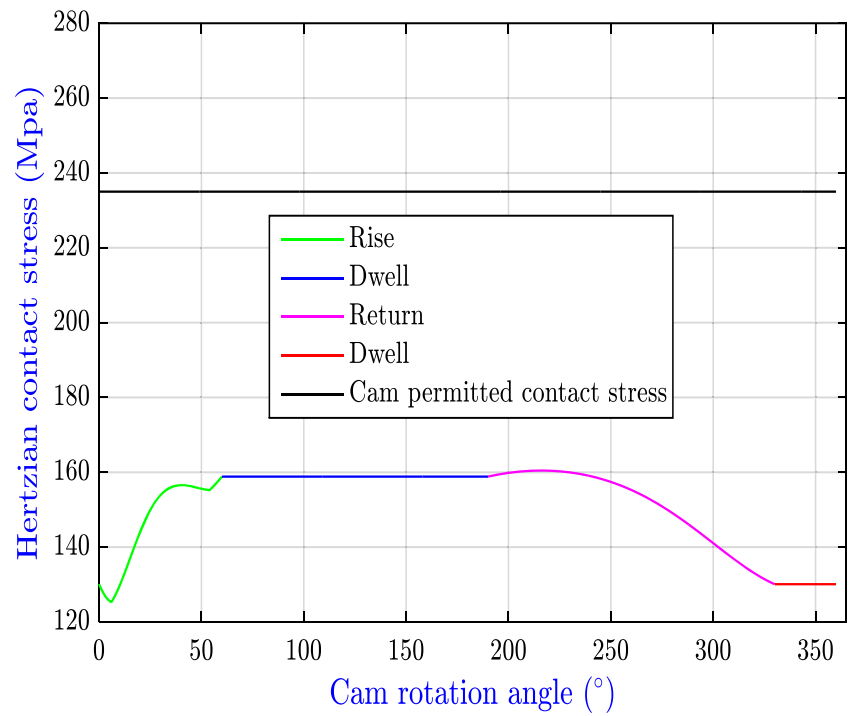
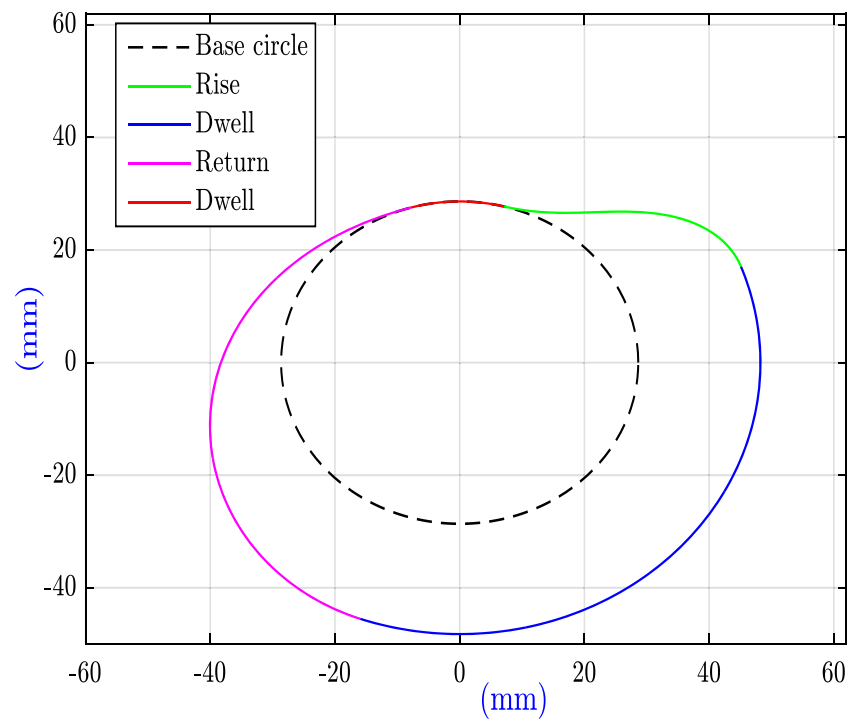


Fig. 16 Optimized cam profile



Funding information This research was supported by the Algerian Ministry of Higher Education and Scientific Research (CNEPRU Research Project No. J0301220110033).

Compliance with ethical standards

Conflict of interest The authors declare that there is no conflict of interest.

Appendix

Three bar truss design

The problem can be mathematically formulated as follows:

$$Min : f(x) = (2\sqrt{2}x_1 + x_2) \times l$$

$$Subject\ to : \begin{cases} g_1(x) = \frac{\sqrt{2}x_1 + x_2}{\sqrt{2}x_1^2 + 2x_1x_2} P - \sigma \leq 0 \\ g_2(x) = \frac{x_2}{\sqrt{2}x_1^2 + 2x_1x_2} P - \sigma \leq 0 \\ g_3(x) = \frac{1}{\sqrt{2}x_2 + x_1} P - \sigma \leq 0 \end{cases}$$

where $0 \leq x_1 \leq 1$, $0 \leq x_2 \leq 1$, $l = 100$ cm, $P = 2$ kN, $\sigma = 2$ kN/cm²

$$\tau(x) = \sqrt{(\tau')^2 + (\tau'')^2 + 2\tau'\tau''\frac{x_2}{2R}}, \tau' = \frac{P}{\sqrt{2}x_1x_2}, \tau'' = \frac{MR}{J}, M = P\left(L + \frac{x_2}{2}\right),$$

$$R = \sqrt{\frac{x_2^2}{4} + \frac{(x_1 + x_3)^2}{4}}, J = 2 \left\{ \sqrt{2}x_1x_2 \left[\frac{x_2^2}{12} + \frac{(x_1 + x_3)^2}{4} \right] \right\}, \sigma(x) = \frac{6PL}{x_4x_3^2},$$

$$P_c(x) = \frac{4.013E\sqrt{x_3^2x_4^6/36}}{x_4x_3^2} \left(1 - \frac{x_3}{2L} \sqrt{\frac{E}{4G}} \right),$$

$P = 6000$ lp, $l = 14$ in, $G = 12 \times 10^6$ psi, $E = 30 \times 10^6$ psi, $\tau_{max} = 13,600$ psi, $\sigma_{max} = 30,000$ psi,
 $\delta_{max} = 0.25$ in
 $0.1 \leq x_1, x_4 \leq 2, 0.1 \leq x_2, x_3 \leq 10$

Tension spring design problem

The problem can be mathematically formulated as follows:

$$Min f(x) = (x_3 + 2)x_2x_1^2$$

$$Subject\ to : \begin{cases} g_1(x) = 1 - \frac{x_2^3x_3}{71785x_1^4} \leq \\ g_2(x) = \frac{4x_2^2 - x_1x_2}{12566(x_2x_1^3 - x_1^4)} + \frac{1}{5.108x_1^2} \leq 0 \\ g_3(x) = 1 - \frac{140.45x_1}{x_2^2x_3} \leq 0 \\ g_4(x) = \frac{x_2 + x_1}{1.5} - 1 \leq 0 \end{cases}$$

where $0.05 \leq x_1 \leq 2$, $0.25 \leq x_2 \leq 1.3$, $2 \leq x_3 \leq 15$

Welded beam design problem

The problem can be mathematically formulated as follows:

$$Min f(x) = 1.10471x_1^2x_2 + 0.04811x_3x_4(14.0 + x_2)$$

$$Subject\ to : \begin{cases} g_1(x) = \tau(x) - \tau_{max} \leq 0 \\ g_2(x) = \sigma(x) - \sigma_{max} \leq 0 \\ g_3(x) = x_1 - x_4 \leq 0 \\ g_4(x) = 0.1047x_1^2 + 0.04811x_3x_4(14 + x_2) - 5 \leq 0 \\ g_5(x) = 0.125 - x_1 \leq 0 \\ g_6(x) = \delta(x) - \delta_{max} \leq 0 \\ g_7(x) = P - P_c(x) \leq 0 \end{cases}$$

where

Publisher’s Note Springer Nature remains neutral with regard to jurisdictional claims in published maps and institutional affiliations.

References

- Hirschhorn J (1962) Pressure angle and minimum base radius. Mach Des 34:191–192
- Fenton RG (1966) Determining minimum cam size. Mach Des 38(2):155–158
- Terauchi Y, El-Shakery SA (1983) A computer-aided method for optimum design of plate cam size avoiding undercutting and separation phenomena. Mech Mach Theory 18(2):157–163
- Bouzakis KD, Mitsi S, Tsiafis I (1997) Computer aided optimum design and NC milling of planar cam mechanisms. Int J Mach Tool Manu 37(8):1131–1142
- Carra S, Garziera R, Pellegrini M (2004) Synthesis of cams with negative radius follower and evaluation of the pressure angle. Mech Mach Theory 39:1017–1032
- Lampinen J (2003) Cam shape optimization by genetic algorithm. Comput Aided Des 35:727–737

7. Tsiafis I, Paraskevopoulou R, Bouzakis KD (2009) Selection of optimal design parameters for a cam mechanism using multi-objective genetic algorithm. *Annals of the Constantin Brancusi, University of TarguJiu, Romania, Engineering series 2*: 57–66
8. Tsiafis I, Mitsi S, Bouzakis KD, Papadimitriou A (2013) Optimal design of a cam mechanism with translating flat-face follower using genetic algorithm. *Tribol Ind* 35(4):255–260
9. Flores P (2013) A computational approach for cam size optimization of disc cam follower mechanisms with translating roller followers. *J Mech Robot* 5:041010–041016
10. Hidalgo-Martinez M, Sanmiguel-Rojas E, Burgos MA (2014) Design of cams with negative radius follower using Bézier curves. *Mech Mach Theory* 82:87–96
11. Hidalgo-Martinez M, Sanmiguel-Rojas E (2015) Minimization of the sliding velocity in planar cam mechanisms with flat-faced translating followers. *Proc Inst Mech Eng C J Mech Eng Sci* 231(9): 1632–1638
12. Jana RK, Bhattacharjee P (2017) A multi-objective genetic algorithm for design optimisation of simple and double harmonic motion cams. *Int J Design Engineering*. <https://doi.org/10.1504/IJDE.2017.089639>
13. Yu Q, Lee HP (1998) Size optimization of cam mechanisms with translating roller followers. *Proc Inst Mech Eng C J Mech Eng Sci* 212:381–386
14. Rothbart HA (2004) *Cam design handbook*. McGraw-Hill, New Jersey
15. Chen YF (1982) *Mechanics and design of cam mechanisms*. Pergamon Press, USA
16. Norton RL (2002) *Cam design and manufacturing handbook*. Industrial Press, New York
17. Wilson CE, Salder JP (1993) *Kinematics and dynamics of machinery*, 2nd edn. Harper Collins College Publishers, New York
18. Desai HD, Patel VK (2010) Computer aided kinematic and dynamic analysis of cam and follower. In: *Proceedings of the World Congress on Engineering*, vol 2. London, pp 117–127
19. Stom R, Price K (1997) Differential evolution—a simple and efficient adaptive scheme for global optimization over continuous spaces. *J Glob Optim* 11(4):341–359
20. Hammoudi A, Djeddou F, Atanasovska I (2017) Adaptive mixed differential evolution algorithm for bi-objective tooth profile spur gear optimization. *Int J Adv Manuf Technol* 90(5–8):2063–2073
21. Brest J, Greiner S, Boskovic B, Mernik M, Zumer V (2006) Self-adapting control parameters in differential evolution: a comparative study on numerical benchmark problems. *IEEE T Evolut Comput* 10:646–657
22. Deb K (2000) An efficient constraint handling method for genetic algorithms. *Comput Methods Appl Mech Eng* 186(2–4):311–338
23. Gong W, Cai Z, Liang D (2014) Engineering optimization by means of an improved constrained differential evolution. *Comput Methods Appl Mech Eng* 268:884–904
24. Mohamed AW, Sabry HZ (2012) Constrained optimization based on modified differential evolution algorithm. *Inf Sci* 194:171–208
25. Mezura-Montes E, Coello CAC, Velázquez-Reyes J, Muñoz Dávila L (2007) Multiple trial vectors in differential evolution for engineering design. *Eng Optim* 39(5):567–589
26. Eskandar H, Sadollah A, Bahreininejad A, Hamdi M (2012) Water cycle algorithm—a novel metaheuristic optimization method for solving constrained engineering optimization problems. *Comput Struct* 110–111:151–166
27. Wang L, Li L (2010) An effective differential evolution with level comparison for constrained engineering design. *Struct Multidiscip Optim* 41:947–963
28. Yi W, Li X, Gao L, Zhou Y, Huang J (2016) ϵ constrained differential evolution with pre-estimated comparison using gradient-based approximation for constrained optimization problems. *Expert Syst Appl* 44:37–49
29. Cuevas E, Cienfuegos M (2014) A new algorithm inspired in the behavior of the social-spider for constrained optimization. *Expert Syst Appl* 41:412–425
30. Nowcki H (1973) Optimization in pre-contract ship design. In: Fujida Y, Lind K, Williams TJ (eds) *Computer applications in the automation of shipyard operation and ship design*, vol 2. Elsevier, New York, pp 327–338
31. Arora JS (1989) *Introduction to optimum design*. McGraw-Hill, New York
32. Rao SS (2009) *Engineering optimization theory and practice*, 4th edn. Wiley, New York
33. Halicioglu R, Dulger LC, Bozdana AT (2017) Modeling, design, and implementation of a servo press for metal-forming application. *Int J Adv Manuf Technol* 91(5–8):2689–2700
34. Halicioglu R, Dulger LC, Bozdana AT (2018) Improvement of metal forming quality by motion design. *Robot Cim-Int Manuf* 51:112–120
35. Pedrammehr S, Danaei B, Abdi H, Masouleh MT, Nahavandi S (2018) Dynamic analysis of Hexarot: axis-symmetric parallel manipulator. *Robotica* 36(2):225–240
36. Caramia M, Dell'Olmo, P (2008) *Multi-objective management in freight logistics: increasing capacity, service level and safety with optimization algorithms*. Springer Verlag London Limited, ISBN: 978–1–84800–381-1